# Raman Spectroscopy Employed for the Determination of the Intermediate Phase in Polyethylene

**Christopher C. Naylor,[†,‡] Robert J. Meier,[†] Bert J. Kip,[†] Kenneth P. J. Williams,[§,∥] Simon M. Mason,[§] Niamh Conroy,[§,⊥] and Don L. Gerrard*[,§]**

*DSM Research, P.O. Box 18, 6160 MD Geleen, The Netherlands, and BP Research Centre, Chertsey Road, Sunbury-on-Thames, Middlesex TW16 7LN, U.K.*

*Received March 19, 1994; Revised Manuscript Received November 25, 1994[⊗]*

ABSTRACT: The original work of Strobl and Hagedorn suggesting the presence of a third intermediate phase in semicrystalline polyethylene was revisited. The current study, involving the collection of Raman spectroscopic data on a set of 16 polyethylene samples recorded on two different types of instruments in two different laboratories and employing two different methods of curve fitting to both sets of experimental data, has revealed that the claims in the original paper cannot be asserted. The most important reason leading to this conclusion is a problem in correctly describing the complicated overlapping spectral structure in the 1000–1200 and 1400–1500 $cm^{-1}$ spectral ranges. It is noted that the contribution of the melt in the 1000–1150 $cm^{-1}$ range cannot be described by a single line centered around 1080 $cm^{-1}$. The present results indicate that the quantification of a third, intermediate, phase in polyethylene is not possible when based on standard Raman spectra.

## Introduction

For more than a decade considerable attention has been paid to the, possible, existence of a third phase in semicrystalline homopolymers, forming an interfacial layer between the crystalline and the amorphous material. In recent reviews Mandelkern[1,2] concluded that the latest theoretical and experimental developments have effectively solved this problem; i.e. an interfacial region of bulk-crystallized homopolymers has been proven to exist. The first studies related to the possible existence of such a third phase were reported by Bergmann and Nawotki[3] and Kitamara et al.[4,5] employing proton NMR and by Strobl and Hagedorn[6] employing Raman spectroscopy. Similar conclusions were formulated by employing these and various other techniques, including NMR[7–10] (both proton NMR and $^{13}C$ NMR), neutron scattering,[11] specific heat,[12,13] dielectric relaxation,[14,15] small angle X-ray scattering,[15,16] and Raman scattering,[17,18] as well as from analysis of molecular simulations.[19–21] Whereas Cheng et al.[12,13] introduced the concept of "rigid amorphous", later this structure was identified as the third phase of interfacial material.[15]

With respect to the relevance of the existence of a third phase, the introduction of a third phase with different mechanical properties (modulus, tensile strength) tends to enable the fitting of experimental mechanical data where two-phase parallel or series models fail. The fraction of intermediate phase is generally used as a parameter to fit the data. If spectroscopy were able to determine the fraction of third phase in the material, this would be one step further toward a solid foundation of describing the mechanical properties of semicrystalline homopolymers with a three-phase model.

Although the recent literature suggests that the existence of the intermediate phase has been proven, we had some doubts with respect to employing the method that uses Raman spectroscopy for this purpose, as it was first proposed by Strobl and Hagedorn. The latter method does not seem to involve a proper and rigorous manipulation of the experimental data. Moreover, the independence of the resulting fractions of third-phase material has not been verified as being independent of both the type of Raman instrument and the subsequent data manipulation, while using the same set of samples.

In the present study we have focused on the Raman method for determining the interfacial fraction as first proposed by Strobl and Hagedorn.[6] According to these authors, if polyethylene were simply a two-phase structure, it should be possible to synthesize the Raman spectrum of a sample of semicrystalline polyethylene from a weighted sum of the spectrum of a model crystalline compound and of a model amorphous compound, i.e., a completely molten polyethylene. Figure 1 shows a typical Raman spectrum from a low-density polyethylene in the 700–1650 $cm^{-1}$ spectral region. The Raman spectrum of polyethylene in the range 1000–1600 $cm^{-1}$ can be subdivided into three main regions (for assignments see refs 22–24): (1) C–C stretching vibrations in the 1000–1150 $cm^{-1}$, region, (2) $-CH_2-$ twisting vibrations at ca. 1300 $cm^{-1}$, and (3) $-CH_2-$ deformation, among which wagging, vibrations between 1350 and 1500 $cm^{-1}$.

Strobl and Hagedorn found that superposition of a crystalline spectrum and an amorphous spectrum yields the spectrum of semicrystalline polyethylene in regions 1 and 2, whereas it fails to do so in region 3. They concluded that this analysis that this implies the presence of the third, interfacial, region. By noting that only the band at 1440 $cm^{-1}$ and the cluster at ca. 1300 $cm^{-1}$ are present in the melt spectrum, whereas the band at 1415 $cm^{-1}$ is only observed in relation to (orthorhombic) crystalline polyethylene, Strobl and Hagedorn defined their three-phase model as follows: (i) an orthorhombic crystalline phase, (ii) an amorphous

* To whom correspondence should be addressed.
† DSM Research.
‡ On leave from Chemistry Department, University of York, York YO1 5DD, U.K.
§ BP Research Centre.
∥ Present address: Renishaw Ltd., Transducer Systems Division, Old Town, Wotton-under-Edge GL12 7DH, U.K.
⊥ Present address: Birds Eye/Walls, Ladysmith Road, Grimsby, South Humberside DN32 9SF, U.K.
⊗ Abstract published in *Advance ACS Abstracts,* February 1, 1995.

0024-9297/95/2228-2969$09.00/0 © 1995 American Chemical Society

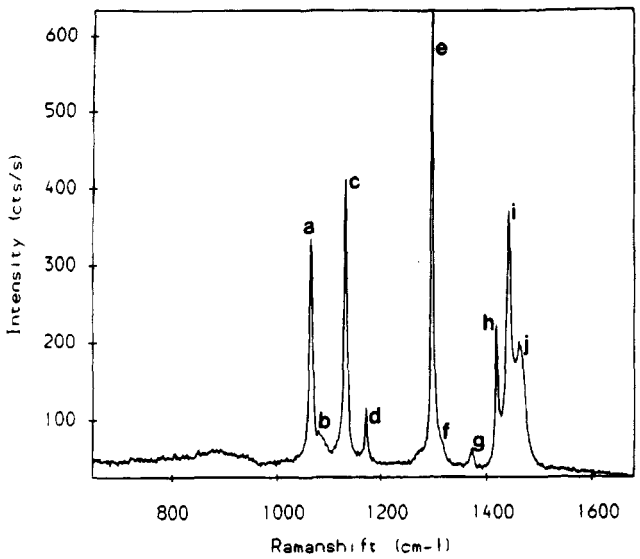


**Figure 1.** Typical Raman spectrum from an LDPE sample (700–1700 $cm^{-1}$), recorded with the grating spectrometer. The Raman band positions and assignments according to the literature[18–20] are as follows: (a) 1060 $cm^{-1}$ asymmetric C–C stretching, crystalline; (b) 1080 $cm^{-1}$ (band center) C–C stretching band in amorphous polyethylene; (c) 1130 $cm^{-1}$ symmetric C–C stretching, crystalline; (d) 1170 $cm^{-1}$ $CH_2$ rocking, crystalline; (e) 1295 $cm^{-1}$ $CH_2$ twisting, crystalline; (f) 1305 $cm^{-1}$ $CH_2$ twisting; amorphous counterpart of 1295 $cm^{-1}$ crystalline band; (g) 1360 $cm^{-1}$ $CH_2$ bending, both crystalline and amorphous; (h) 1415 $cm^{-1}$ $CH_2$ wagging, crystalline; (i) 1440 $cm^{-1}$ $CH_2$ deformation, both crystalline and amorphous; (j) 1470 $CH_2$ bending, both crystalline and amorphous.

phase with a structure strongly resembling the melt, and (iii) an interfacial region between the crystalline and the amorphous phase consisting of crystalline-like structures which have lost their lateral order but cannot simply be characterized as another crystal modification.

The next logical step taken by Strobl and Hagedorn was to determine if the content of each of these three phases could be calculated directly from analysis of the Raman spectra. They concluded that the fractions of the different phases of the polymer can be determined from the intensity of particular bands, with *all* band intensities $I_x$ being taken *relative to* the total integrated intensity of the $CH_2$ twisting bands, i.e. the bands in the 1295–1305 $cm^{-1}$ region. The crystalline fraction, $\alpha_c$, is determined directly from the relative intensity of the $CH_2$ bending model at 1415 $cm^{-1}$ by employing the equation $\alpha_c = I_{1415}/0.46$.[6] The amorphous fraction $\alpha_a$ can be obtained in two ways. The first is from the relative intensity of the broad $CH_2$ twisting band centered at 1305 $cm^{-1}$, employing the relation $\alpha_a = I_{1305}$. The alternative is to calculate $\alpha_a$ from the relative intensity of the amorphous C–C stretching band at 1080 $cm^{-1}$, according to the relation $\alpha_a = I_{1080}/0.79$. The fraction of the interfacial region $\alpha_b$ is given by the difference between unity and the sum of the fractions in the amorphous and crystalline regions, i.e. $\alpha_b = 1 - \alpha_a - \alpha_c$. The values 0.46 and 0.79 are normalization constants derived from spectra obtained from a 100% crystalline paraffin sample and from the polyethylene melt, respectively. The former value arises from the relative intensity of the 1415 $cm^{-1}$ band,[6] whereas the factor 0.79 was derived from the ratio of the intensity of the 1080 $cm^{-1}$ band in the melt to the total intensity of the $CH_2$ twisting band in the 1296–1305 $cm^{-1}$ region.

This initial work was supplemented by further studies by Glotin and Mandelkern.[25] More recently, Failla et al.[26] have employed computerized fitting using the LabCalc software program (Galactic Industries) describing the Raman bands as sums of a Lorentzian and a Gaussian band shape. These authors concluded that manual deconvolution was as good as computerized analysis of the Raman spectra, but the curve-fitting procedure was only tested in the spectral region 1240–1350 $cm^{-1}$ and thus did not incorporate the 1080 and 1415 $cm^{-1}$ bands employed by Strobl and Hagedorn to calculate the normalization constants 0.79 and 0.46. Wang et al.[27] have used the method to study the morphology of polyethylene reactor powder and reported that spectral differences and hence crystallinity differences could be monitored. Keresztury and Foldes[28] used mathematical curve-fitting procedures to quantify their Raman intensities. However, they used simple Gaussian–Lorentzian sum functions without taking into account spectrometer broadening and did not study the spectra of model crystalline and model amorphous compounds. Rull et al.[18] proposed an alternative method based on time-dependent Fourier deconvolution of the spectral region between 950 and 1500 $cm^{-1}$ for obtaining the relative amount of the three phases. They have argued that previous assessments (using Raman spectra) of the amorphous content of polyethylene were overestimates and that a careful analysis of both baseline corrections and an accounting for shoulders has to be carried out. Very recently, Mutter et al.[17] claimed that the analysis of the Raman spectra of semicrystalline polyethylene leads to the characterization of *four* different phases. The extra fourth phase was characterized as another intermediate phase. In this study, for the first time, the bands were computer-fitted using the Voigt profiles, which is the more appropriate band shape for analyzing solid state Raman bands.

We will not elaborate any further on these recent studies, for during our investigations we identified some basic problems with the methods employed to quantify the third phase in polyethylene using Raman spectroscopy. The purpose of the present paper is to revisit and verify the Strobl and Hagedorn method. In this study we have analyzed a wide range of polyethylene samples. Moreover, for any definite conclusions to be made, we have adopted a previously unemployed requirement, i.e. that conclusions about the existence of a third phase should be independent of the type of instrumentation. For that purpose, data have been acquired using both a grating monochromator based Raman spectrometer (at DSM Research) and a FT-Raman spectrometer (at BP Research) in order to assess the transferability of the method across instrumentation. The FT-Raman technique has not been applied to this problem before, although the advantage of FT-Raman spectroscopy is that essentially no corrections are needed as compared to grating instruments (with use of the latter type of instrument distortions due to the presence of a slit and differences in detector element sensitivity need to be corrected). Special attention has been paid to the line shape distortions that can occur with different data acquisition protocols, and methods have been developed to minimize such effects. In addition two different programs for curve fitting the recorded Raman spectra have been employed.

## Materials and Methods

**Samples.** Polyethylene samples were chosen to encompass a wide range of density (crystallinity) values from 0.963 to 0.904 kg $m^{-3}$ (37–78 mass % crystallinity).

The set consisted of eight high-density polyethylenes (HDPE's), four linear low-density polyethylenes with controlled short branching (LLDPE's), three low-density polyethylenes with both short and long chain branching (LDPE's), and a very low density polyethylene (VLDPE). In addition a set of model compounds were studied incorporating $C_{36}H_{74}$, $C_{58}H_{118}$, and $C_{198}H_{398}$.

**Instrumentation.** All facts relating to recording the spectra are according to the following unless detailed otherwise.

Raman spectra were recorded at DSM Research using a Jobin-Yvon U1000 spectrometer fitted with 600 grooves/mm gratings (spectral coverage ca. 600 $cm^{-1}$) employing 514 nm excitation wavelength (Spectra Physics model 2025 $Ar^+$ laser) and using a 1024 pixel intensified diode array. A microscope with a ×20 objective (5 $\mu$m diameter laser spot size) was interfaced. In order to correct for the differences in sensitivity of the elements of the diode array the response to a white light source was recorded and employed in correcting the experimental polyethylene Raman spectra. Laser powers at the sample were kept low (5−10 mW) to avoid sample heating.[29] The main sources of instrumental spectral broadening arise from the slit of the grating monochromator system and from the cross talk between the pixels of the diode array. It will be explained in the next subsection how this instrumental broadening was accounted for. Data were recorded at a spectral resolution of ca. 2 $cm^{-1}$ using a slit width of 100 $\mu$m. Because of the small spot size, sample inhomogeneities might seriously affect the Raman spectrum obtained. This was carefully checked by (1) recording spectra from different locations on the sample and, whenever necessary, averaging these spectra, or (2) whenever applicable, depolarizing the incoming laser beam in order to minimize the effects of preferred chain orientation in the probed sample volume. The depolarization was achieved by placing a polarization scrambler ($\lambda/4$ plate) before the monochromator entrance slit.

Raman data were recorded from an identical sample set at BP Research using a FT-Raman spectrometer (Perkin-Elmer) that has been described in full elsewhere.[30] Samples were investigated using a softly focused Nd:YAG laser (300 $\mu$m spot diameter) operating at 1.064 $\mu$m with an incident power of ca. 200 mW. The interferometer, optimized for the near-infrared spectral range, was used with a liquid nitrogen cooled InGaAs detector. The only significant source of spectral broadening in the system is the line width of the laser which was of the order of 0.5 $cm^{-1}$. Spectra were recorded using 2 $cm^{-1}$ spectral resolution and boxcar apodization. Under these conditions it has been previously shown that instrumental response is good and free of spectral distortion.[31] Data recorded from the FT-Raman spectrometer were corrected for white light response.

The measurements at elevated temperatures were performed by positioning the sample in a Linkam Instruments TMS 91 hot stage, placed on the microscope stage. A ×50 long-working distance objective was used. The laser spot on the sample was about 2 $\mu$m. Nitrogen gas was purged over the sample in order to avoid oxidation at elevated temperatures. Equivalent data could not be obtained with the FT-Raman instrument owing to problems of black body emission interference observed at a temperature of 140 °C.

**Curve Fitting.** The curve fitting of our data was achieved in two ways to assess the transferability of the methods and the effect this had on our final values of

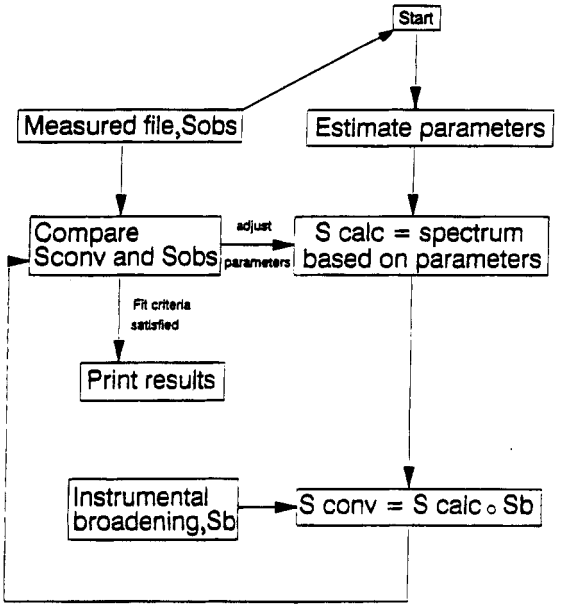


**Figure 2.** Flow sheet explaining the procedure for the iterative fitting of Raman spectra employing the in-house developed software program ("Voigt"). $S_{obs}$ stands for the experimentally recorded Raman spectrum, $S_{calc}$ for the synthesized Raman spectrum with instrumental broadening not yet accounted for, $S_b$ for the instrumental broadening spectrum as experimentally recorded on narrow spectral lines, and $S_{conv}$ for the convolution of the instrumental broadening spectrum and the synthesized spectrum $S_{calc}$. For further explanation see text.

Raman crystallinity. (i) Data were fitted using the routine found in the SpectraCalc software package (Galactic industries) which provides a summation of appropriate amounts of Gaussian and Lorentzian profiles. This method will from now on be referred to as "SpectraCalc". (ii) Data were subjected to an in-house developed program based on an IMSL routine for nonlinear least squares fitting based on the Levenberg−Marquardt algorithm. This program uses Voigt line shapes[32] (convolution of Lorentzian and Gaussian band shapes) to describe the bands. This method will from now on be referred to as "Voigt". In the actual curve fitting, using either of the two routines, the background was fitted simultaneously with the Raman bands. The background was assumed to vary linearly with the Raman shift.

For the purpose of manipulating the Raman spectroscopic data recorded on the grating instrument, the self-assembled fit program using the Voigt band shape was adapted to remove the effect of instrumental broadening. This was accomplished by first calculating the convolution of the synthesized Raman spectrum (Voigt functions of individual Raman bands plus background) and the experimentally determined instrumental broadening function (the determination of the latter is to be discussed later). This result was subsequently compared to the experimental spectrum recorded on the grating instrument (see Figure 2), and appropriate changes were made iteratively to the band parameters substituted in the fitting program until optimum agreement between the experimental and synthesized spectra was obtained. To circumvent unwanted artefacts, this procedure was preferred over a procedure involving deconvolution of the original Raman spectrum with the instrument function.

Normally, both of the fitting routines were run with all parameters free. Constraints needed to be imposed

when fitting very weak and broad spectral features. In particular, problems of this nature became very apparent in data recorded from the high-density samples which contained a relatively small amount of amorphous material. These data provided broad spectral features that often merged into the overall background levels.

## Results and Discussion

A primary concern was establishing spectral acquisition protocols and curve-fitting procedures that were reliable and provided uniformity across different sampling and instrumentation. The first step involved the determination of the instrument broadening characteristics of the grating instrument by using an intrinsically narrow spectral line, for which purpose a mercury lamp emission line at 546 nm (1122 $cm^{-1}$ from 514.5 nm) and the plasma line from the argon laser at 3233 $cm^{-1}$ were used. Data were obtained at a range of slit widths. Because the spectra obtained could not be fitted well with a single Voigt function, the actual numerical set of data points were used as what we call the instrumental broadening function $S_b$, and subsequently employed in the spectral-fitting procedure outlined in Figure 2.

To *test* the fitting procedure developed (cf. Figure 2), including the instrumental broadening file, we used a sample which exhibited a well-defined narrow Raman line that contained little or no spectral interferences or overlaps. Potassium nitrate, ground to a fine powder, was used to provide a single intense line at 1048 $cm^{-1}$. Data were obtained using the grating instrument with slit widths varying from 50 to 200 $\mu$m. The optimal conditions for acquiring data were found at the 100 $\mu$m slit width. Above a slit width of 100 $\mu$m significant spectral broadening and band shape distortion occurred. Using this slit width, the nitrate band of a $KNO_3$ solution could be curve fitted using the instrumental broadening files and Voigt profiles to provide a 100% Lorentzian shape with a HWHH (half-width at half-height) of 3.18 $cm^{-1}$. The same sample run on the FT-Raman system could be fitted with a 100% Lorentzian line shape and a line width of 3.22 $cm^{-1}$ (HWHH). The agreement between the two data sets is excellent and it is concluded that under these acquisition conditions one can be very confident of not introducing artefacts into the band shapes of the spectra as a result of the spectrum acquisition procedure.

Next, a series of well-defined model alkane compounds was investigated. This assessed the potential problems with the recording and curve fitting of the Raman data from linear alkanes and also served to verify the normalization constants derived by Strobl,[6] i.e. the numerical values 0.46 and 0.79 quoted in the Introduction. Figure 3 illustrates the spectra obtained from the $C_{36}H_{74}$ sample recorded using the grating Raman instrument (Figure 3a) and the FT-Raman spectrometer (Figure 3b). The two spectra are essentially the same and are typical of the recorded spectra over the entire set of alkanes studied. Table 1 lists the ratios of the 1060, 1130, and 1415 $cm^{-1}$ bands and the 1440–1480 $cm^{-1}$ region relative to the integrated intensity of the 1295 $cm^{-1}$ band for both the $C_{36}H_{74}$ and the $C_{58}H_{118}$ model compounds. Also listed in the table are the band widths (HWHH) measured from the individual bands. The relative areas given in Table 1 when using the in-house developed fitting routine were calculated by taking into account the

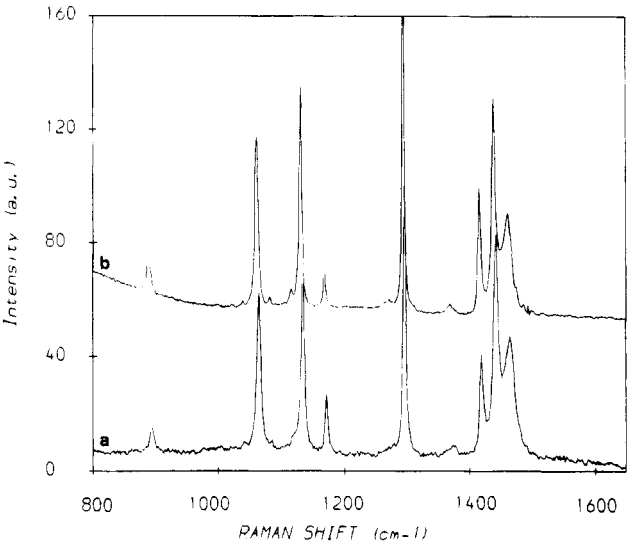


**Figure 3.** Raman spectrum recorded from $C_{36}H_{74}$ using (i) conventional Raman instrumentation, 514.5 nm excitation, and (ii) FT-Raman, 1.064 $\mu$m excitation.

instrumental broadening function for the spectra recorded with the grating instrument without depolarizing the incoming laser beam ($C_{198}$ (ext) sample, last column Table 1). In the course of our studies and after extensive experience with the effect of the instrumental broadening function on the fitting results, including derived areas, it was found that, rather than using the procedure outlined in Figure 2, the instrumental broadening could be equally well described by fixing an additional Gaussian width (width = 1.1 $cm^{-1}$) in the Voigt profile. As we experienced, the main reason why this gave a result equally satisfactory to that following from applying the method outlined in Figure 2 in accounting for the instrumental broadening function was that the very broad amorphous bands could not be fitted to the desired degree of accuracy. This led to discrepancies in final values for, e.g., crystallinities that were much larger than those errors introduced when not accounting for instrumental broadening in the most explicit way, i.e. along the lines of Figure 2. All Raman bands (after correction for instrumental broadening by applying this fixed Gaussian band width) could be described very well by pure Lorentzian band shapes. As a consequence, all other numbers in Table 1 were obtained by employing a convolution of a variable Lorentzian band and a Gaussian band with fixed band width (1.1 and 1.4 $cm^{-1}$ for the grating and the FT instrument, respectively). Despite this finding, it is to be emphasized that the initial procedure outlined in Figure 2 involving the experimental broadening file was considered necessary as a primary test, whereas the alternative procedure was only used when it was found to yield equivalent results.

Returning to the data presented in Table 1, it is observed that whereas mutual agreement between calculated band areas for both the FT-Raman and the grating spectrometer recorded spectra, using either of the two fit routines (SpectraCalc or Voigt), is very good for the 1060, 1130, and 1415 $cm^{-1}$ bands, it is much worse for the 1440–1480 $cm^{-1}$ region. For the latter region the two curve-fitting routines still provide reasonable agreement when applied to either the grating instrument spectra or to the FT-Raman spectra, *but a substantial difference is observed between the results obtained from the different spectrometer types.*

**Table 1. Comparison of Band Areas and Band Widths for the Model Alkane Crystalline Compounds $C_{36}H_{74}$, $C_{58}H_{118}$, and Extended $C_{198}H_{398}$ As Calculated with the Two Different Fitting Routines (Voigt and Spectracalc) and Applied from the Spectra As Obtained from the Grating Instrument as Well as from the FT-Raman Instrument**

| | sample | | | | | | | | |
|---|---|---|---|---|---|---|---|---|---|
| | $C_{36}H_{74}$ | | | | $C_{58}H_{118}$ | | | | $C_{198}$(ext) grating |
| | grating | | FT-Raman | | grating | | FT-Raman | | |
| | Voigt | SpectraCalc | Voigt | SpectraCalc | Voigt | SpectraCalc | Voigt | SpectraCalc | Voigt |
| | Area Relative to the Band at 1295 $cm^{-1}$ | | | | | | | | |
| 1060 | 0.80 | 0.79 | 0.78 | 0.80 | 0.76 | 0.76 | 0.76 | 0.76 | 0.76 |
| 1130 | 0.72 | 0.73 | 0.81 | 0.79 | 0.82 | 0.86 | 0.85 | 0.91 | 0.87 |
| 1415 | 0.42 | 0.41 | 0.41 | 0.41 | 0.43 | 0.46 | 0.39 | 0.44 | 0.44 |
| 1440 | 2.89 | 2.88 | 2.02 | 2.00 | 2.29 | 2.26 | 2.12 | 2.13 | 2.29 |
| | Total Width of the Band ($cm^{-1}$) | | | | | | | | |
| 1060 | 4.3 | 3.7 | 3.8 | 3.2 | 4.1 | 3.6 | 3.5 | 3.0 | 3.5 |
| 1130 | 3.9 | 3.1 | 3.0 | 2.5 | 4.0 | 3.3 | 3.1 | 2.5 | 3.3 |
| 1295 | 3.1 | 2.5 | 2.2 | 1.8 | 3.0 | 2.5 | 2.3 | 1.9 | 2.5 |
| 1415 | 4.3 | 3.7 | 3.3 | 2.6 | 3.8 | 3.3 | 3.3 | 2.7 | 3.1 |

In addition to these results, the agreement across the different approaches was not initially as good for each of the model compounds studied. Using micro Raman methods to measure the Raman data from the grating instrument, nonreproducible values for the calculated relative band areas were obtained. This was found to be due to polarization effects from the analysis of small crystals in different local orientations. To avoid this problem, a polarization scrambler was introduced in the exciting laser beam. Problems with sample inhomogeneity were also encountered, which were overcome by running a series of spectra from different areas on the sample and averaging the spectra. Taking these precautions, the analysis of the data from the model compounds showed that the original figure of 0.46 calculated by Strobl[6] for the ratio of the intensities of the 1415 and 1295 $cm^{-1}$ bands was found to be slightly lower, i.e. 0.43.

To assess the validity of the other normalization constant used in the method of Strobl and Hagedorn, i.e. the value of 0.79 relating to the relative intensity of the amorphous 1080 $cm^{-1}$ band, data were collected from a sample of $C_{36}H_{74}$ at a range of temperatures between 65 and 150 °C (Figure 4a–f), together with a spectrum recorded from a linear low-density polyethylene sample at 140 °C (Figure 4g). The melting temperatures of $C_{36}H_{74}$ and the LLDPE are 76 and 129 °C, respectively. It can be seen from Figure 4a–f that once the melt temperature is achieved very dramatic spectral changes are observed. The triplet band centered at 1440 $cm^{-1}$ becomes broadened, as does the band around 1300 $cm^{-1}$. The two peaks seen at 1060 and 1130 $cm^{-1}$ in the solid state disappear to leave a broad triangular-shaped band at 1080 $cm^{-1}$, together with a weak broad feature at 1130 $cm^{-1}$. These are all well-known features, related to crystalline bands disappearing and melt- or amorphous-like bands becoming more intense. The most dramatic spectral change seems to occur outside the region most commonly used to probe the polyethylene morphology. After the melt temperature is achieved, a very strong and broad band is seen centered at 870 $cm^{-1}$, which some have attributed[17] (original assignment by Gall et al.[24]) to $CH_2$ rocking vibrations in polyethylene with coiled chains, whereas others[33] have attributed this band to delocalized C–C stretch vibrations. We do not further discuss this feature for it is not of particular relevance to the present investigation. Similar Raman spectra were obtained from both high and low-density polyethylene samples. No qualitative differences were found between the various polymer melt spectra taken at different temperatures, ranging from 140 up to 250 °C. In contrast to the suggestions in ref 6, the present results unambiguously revealed that the Raman spectra of melts of polyethylene as well as from the model compounds cannot be described by single Raman bands at 1080, 1305, and 1440/1450 $cm^{-1}$. Figure 5 illustrates a typical curve fit of the Raman spectrum recorded from a low-density polyethylene at 198 °C, demonstrating the fact that the band centered at 1440 $cm^{-1}$ requires a minimum of two bands to synthesize the line shape. The band at 1305 $cm^{-1}$ can be well fitted with a single component. However, extreme difficulty was encountered when trying to fit the 1080 $cm^{-1}$ Raman band with a single Voigt band. In Figure 5 we show that this portion of the spectrum can only be fitted by using at least two components. During the investigations it became clear that the band at 1080 $cm^{-1}$ is a complex convolution of at least three components with peaks at 1020, 1060, and 1080 $cm^{-1}$. Some of the previous authors have found it necessary to take into account an extra band centered around 1020 $cm^{-1}$ (see Keresztury and Földes[28] and Rull et al.[18]), surprisingly not mentioned by Mutter et al.[17] and stated as nonproblematic by Glotin and Mandelkern[25] (a single band was assumed by these authors), whereas Failla et al.[26] have only manually deconvoluted this region of the Raman spectrum. In this respect it is noteworthy to cite Keresztury and Földes[28] who stated that, contrary to the statement by Glotin and Mandelkern, they had experienced great difficulties in the analysis of the 1080 $cm^{-1}$ band. In another place[34] Mandelkern and Peacock did emphasize that the 1080 $cm^{-1}$ band was found to vary in shape and height depending on crystallization conditions. Finally, in the past Snyder[35] has suggested that gauche bond C–C stretching is not involved here, whereas trans can still be a factor. As a consequence a different trans–gauche ratio as a function of, e.g., crystallization conditions but particularly as a function of temperature could seriously affect the band. In summary, the different approaches used in these various studies clearly indicate that, as yet, no consensus has been reached over whether to fit the 1080 $cm^{-1}$ with a single symmetrical band or with more than one band. As a consequence of the complex band shape the fitting of this region in the room temperature spectrum of polyethylenes is equally difficult, with additional (strong) overlap with the crystalline 1060 and 1130 $cm^{-1}$ bands. Consequently, using the 1080 $cm^{-1}$ band for the purpose of quantifying the amount of amorphous material in the

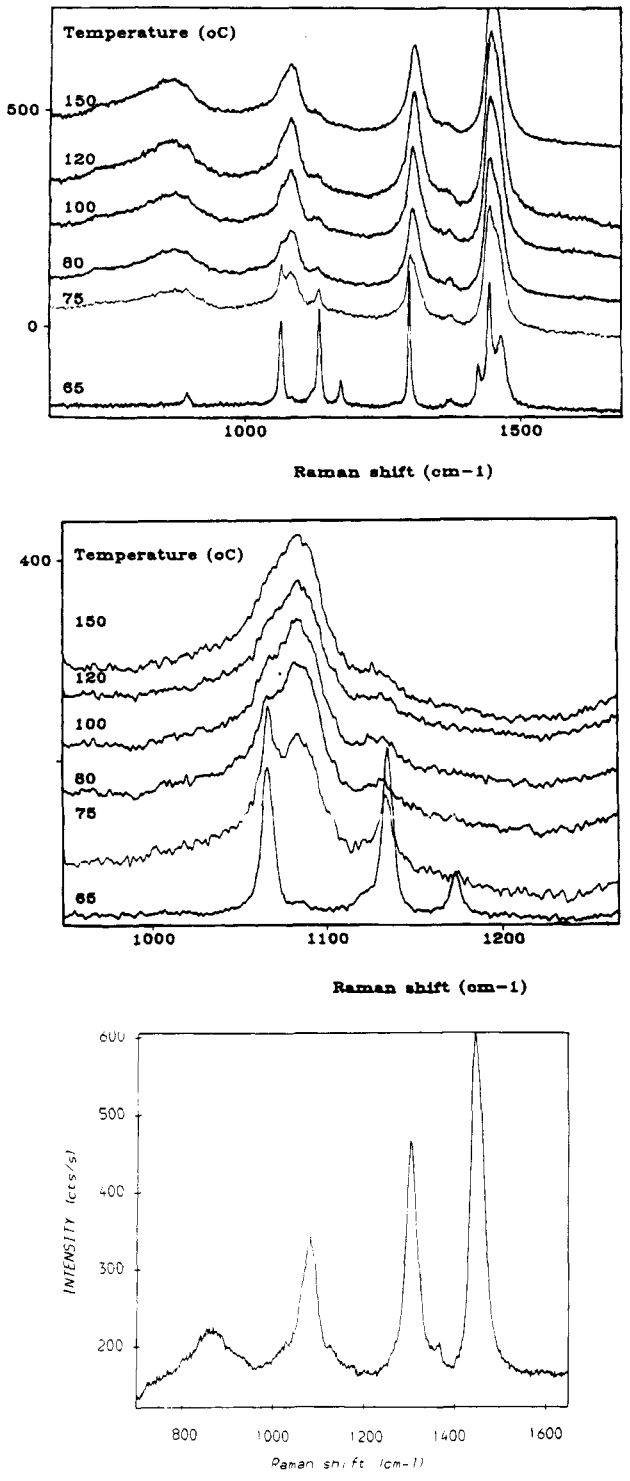


**Figure 4.** Raman data recorded from $C_{36}H_{74}$ at elevated temperatures, using 514.5 nm excitation, and the grating spectrometer: (a) 65 °C, (b) 75 °C, (c) 80 °C, (d) 100 °C, (e) 120 °C, (f) 150 °C. Raman data recorded (g) from LLDPE at 140 °C (bottom spectrum).

polymer is considered highly questionable. In addition, it is doubtful as to whether it is meaningful to assume that this amorphous band at 1080 $cm^{-1}$ should be described by a certain number of symmetrical lines. An alternative is taking the experimental profile of the 1080 $cm^{-1}$ band in the fit; see Mutter et al.[17] and Failla et al.[26]

The most important corollary from these observations is that the normalization constant of 0.79 derived by Strobl and Hagedorn is considered prone to error. This

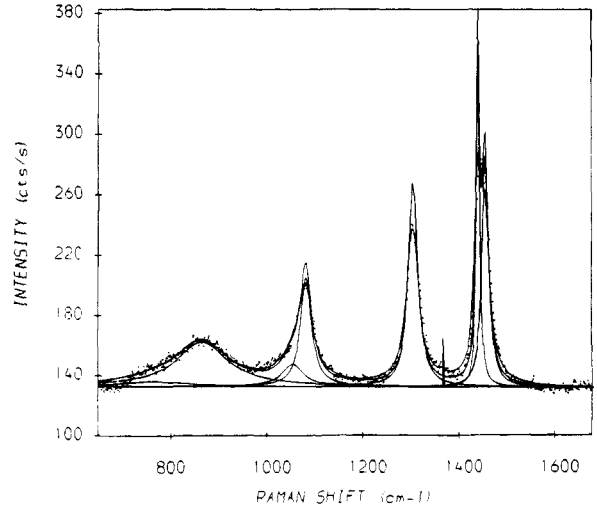


**Figure 5.** Raman spectrum of LDPE recorded at 198 °C compared to the simulated spectrum synthesized from Voigt functions.

is further emphasized by some actual values we calculated on the basis of the Raman spectra of the LLDPE sample with 0.937 $kg/m^3$ density. From the spectrum recorded at 159.0 °C the calculated factor was 0.861, whereas the spectrum recorded at 198.7 °C yielded the value 0.649. In this respect it is noteworthy that in the IR spectra a non-negligible temperature dependence of the intensities has been reported.[36] It is obvious that the method proposed by Strobl and Hagedorn does not account for such effects and that any fraction of third-phase material derived from the relation $\alpha_b = 1 - I_{1415}/0.46 - I_{1080}/0.79$ will suffer from a high uncertainty. *We realize that by stating this, the evidence for the presence of a third phase as based on Raman spectroscopic evidence is seriously questioned.*

In addition to the fitting problems of the melt spectrum, a closer inspection of Figure 4 shows that the strong band at 1130 $cm^{-1}$ seen in the spectrum of the crystalline material becomes progressively weaker and broader as the melt temperature is reached. As far as we know, this observation has not been reported before. However, it is clear that the feature still persists after the melt transition temperature has been reached and is seen as a weak shoulder on the edge of the 1080 $cm^{-1}$ band. A similar feature is also seen in the spectrum of molten linear low-density polyethylene (Figure 4g). In fact, the corresponding figures in the papers by Strobl and Hagedorn[6] and by Mutter et al.[17] also seem to show these features, although no attention was given to them at that time. The origin of the 1130 $cm^{-1}$ band in crystalline polyethylene is well-known and is assigned to the stretching vibration of trans C–C bonds. With the clear observation of the presence of Raman intensity around 1130 $cm^{-1}$, the asymmetry of the 1080 $cm^{-1}$ band toward smaller Raman shifts is most likely due to some residual intensity of the other C–C stretching frequency near 1060 $cm^{-1}$. The observation of this band in the melt is therefore attributed to the presence of short all-trans C–C sequences in the molten polymer. A separate study on this item will be reported elsewhere.[37]

**The 16 Polyethylenes.** We now report on the Raman spectra of all of the 16 polyethylene samples (Table 2). The densities of the polyethylenes cover a wide range. As before, initial experiments were carried out in order to validate the data acquisition methods employed in the present work. Data were recorded from

**Table 2. Crystallinities for the 16 Different Polyethylene Samples Studied in the Present Paper[a]**

| polyethylene | | HDPE (1) | | HDPE (2) | | HDPE (3) | | HDPE (4) | | HDPE (5) | | HDPE (6) | | HDPE (7) | | HDPE (8) | | LLDPE (9) | | LLDPE (10) | | LLDPE (11) | | LDPE (12) | | LDPE (13) | | LDPE (14) | | VLDPE (15) | | LLDPE (16) | |
|---|---|---|---|---|---|---|---|---|---|---|---|---|---|---|---|---|---|---|---|---|---|---|---|---|---|---|---|---|---|---|---|
| % cryst from density (mass) | | 74 | | 75 | | 72 | | 66 | | 67 | | 68 | | 68 | | 68 | | 56 | | 46 | | 46 | | 48 | | 48 | | 46 | | 33 | | 57 | |
| Raman instrument | | grat | FT | grat | FT | grat | FT | grat | FT | grat | FT | grat | FT | grat | FT | grat | FT | grat | FT | grat | FT | grat | FT | grat | FT | grat | FT | grat | FT | grat | FT |
| $I(1130)/I(1060)$ | | 1.20 | 1.02 | 1.17 | 1.03 | 1.17 | 1.09 | 1.22 | 1.06 | 1.24 | 1.07 | 1.30 | 1.08 | 1.26 | 1.03 | 1.17 | 1.03 | 1.14 | 1.13 | 1.16 | 1.03 | 1.09 | 1.05 | 1.12 | 1.05 | 1.10 | 0.98 | 1.10 | 1.05 | 1.03 | 1.16 | 1.18 | 1.05 |
| Voigt fitting proc | % cryst 1415 | 60 | 71 | 67 | 75 | 67 | 66 | 62 | 59 | 60 | 59 | 72 | 61 | 66 | 55 | 51 | 52 | 41 | 42 | 35 | 33 | 28 | 30 | 33 | 32 | 31 | 35 | 30 | 34 | 13 | 17 | 47 | 47 |
| | % cryst 1060 | 67 | 75 | 70 | 76 | 63 | 66 | 60 | 62 | 65 | 72 | 65 | 65 | 64 | 63 | 58 | 63 | 55 | 57 | 47 | 49 | 43 | 46 | 47 | 50 | 51 | 56 | 51 | 56 | 38 | 37 | 58 | 62 |
| | % amorp 1080 | 24 | 25 | 22 | 21 | 23 | 24 | 24 | 26 | 32 | 28 | 28 | 24 | 26 | 24 | 21 | 31 | 37 | 44 | 43 | 45 | 37 | 38 | 36 | 36 | 33 | 38 | 36 | 47 | 40 | 51 | 35 | 35 |
| | % amorp 1305 | 31 | 28 | 24 | 24 | 33 | 34 | 32 | 37 | 34 | 35 | 34 | 38 | 37 | 40 | 40 | 42 | 44 | 47 | 55 | 54 | 58 | 57 | 55 | 60 | 54 | 48 | 54 | 50 | 67 | 64 | 45 | 44 |
| | 100 − ("1415" + "1305") | 9 | 1 | 9 | 1 | −0 | 0 | 6 | 5 | 6 | 6 | −6 | 2 | −3 | 5 | 9 | 6 | 16 | 11 | 11 | 12 | 14 | 12 | 13 | 8 | 15 | 17 | 16 | 16 | 21 | 19 | 8 | 9 |
| | 100 − ("1060" + "1305") | 2 | −3 | 6 | 0 | 4 | 0 | 8 | 1 | 1 | −6 | 1 | −3 | −1 | −3 | 2 | −5 | 2 | −4 | −1 | −4 | −1 | −3 | −1 | −10 | −6 | −4 | −6 | −6 | −5 | −2 | −3 | −6 |
| | "1060" − "1415" | 7 | 4 | 3 | 1 | −4 | 0 | −2 | 4 | 5 | 12 | −7 | 4 | −3 | 8 | 7 | 10 | 14 | 15 | 12 | 16 | 15 | 16 | 14 | 18 | 21 | 21 | 21 | 22 | 25 | 21 | 11 | 15 |
| SpectraCalc fitting proc | % cryst 1415 | | 89 | | 83 | | 68 | | 58 | | 67 | | 58 | | 61 | | 58 | | 50 | | 38 | | 28 | | 39 | | 36 | | 41 | | 20 | | 48 |
| | % cryst 1060 | | 86 | | 78 | | 64 | | 59 | | 67 | | 63 | | 61 | | 59 | | 64 | | 48 | | 41 | | 50 | | 54 | | 62 | | 48 | | 66 |
| | % amorp 1080 | | | | | | | | | | | | | | | | | | | | | | | | | | | | | | | | |
| | % amorp 1305 | | 10 | | 10 | | 32 | | 33 | | 27 | | 43 | | 41 | | 41 | | 28 | | 51 | | 55 | | 56 | | 52 | | 46 | | 66 | | 41 |
| | 100 − ("1415" + "1305") | | 1 | | 7 | | 0 | | 9 | | 6 | | −1 | | −2 | | 1 | | 22 | | 11 | | 17 | | 5 | | 12 | | 13 | | 14 | | 11 |
| | 100 − ("1060" + "1305") | | 4 | | 12 | | 4 | | 8 | | 6 | | −6 | | −2 | | 0 | | 8 | | 1 | | 4 | | −6 | | −6 | | −8 | | −14 | | −7 |
| | "1060" − "1415" | | −3 | | −5 | | −4 | | 1 | | 0 | | 5 | | 0 | | 1 | | 14 | | 10 | | 13 | | 11 | | 18 | | 21 | | 28 | | 18 |

[a] The crystallinities calculated from density (mass crystallinity) are given for reference purposes, whereas the other values are percentages reflecting the fraction of the material that is crystalline or amorphous, respectively, as calculated on the basis of the Raman bands indicated. "grat" stands for data obtained from the Raman spectra recorded with the grating instrument, and "FT" for similar data obtained using the FT-Raman spectrometer. Details on the two curve-fitting procedures, i.e. "Voigt" and "SpectraCalc" are explained in the text.

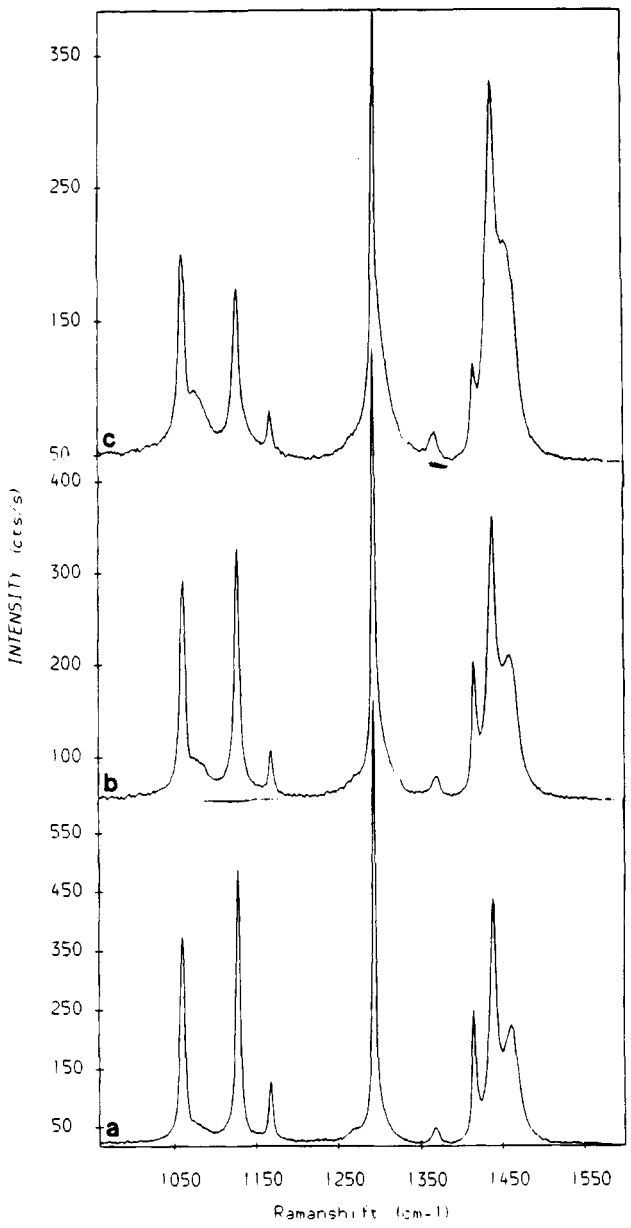


**Figure 6.** Raman spectra from a range of polyethylene samples as recorded on the grating instrument using 514.5 nm excitation: (a) HDPE, density 0.964; (b) LDPE, density 0.936; (c) VLDPE, density 0.904 kg/m$^3$.

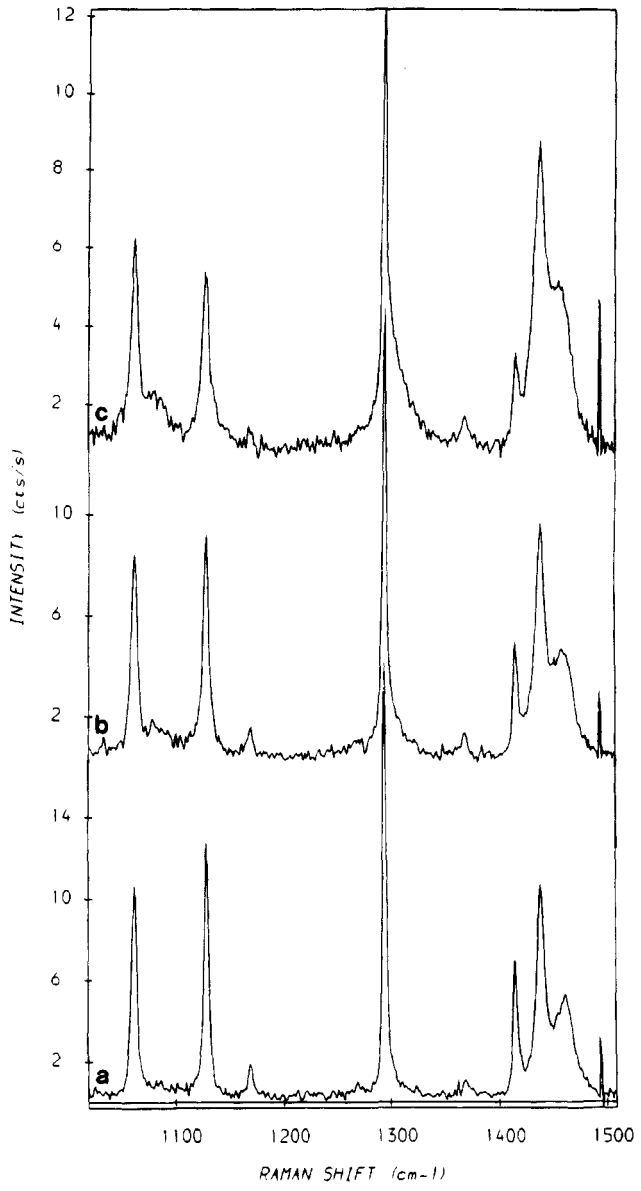


**Figure 7.** Spectra as in Figure 6, recorded on the FT-Raman instrument, using 1.064 $\mu$m excitation.

a high- and low-density polyethylene sample at a range of incident laser powers to assess the effect this may have on the spectra (laser-induced heating). It was seen that at high laser powers (>25 mW), using 514.5 nm laser excitation and the micro attachment, some laser annealing of the polymer occurred that caused changes in the Raman spectrum. For this reason the laser powers used in this experiment were restricted to between 5 and 15 mW at the sample with the ×20 objective. A similar set of experiments using the FT-Raman instrument using a defocused laser spot showed no signs of laser damage to the sample even at powers of 500 mW.

Figures 6 and 7 show the spectra of three of the polyethylene samples recorded with the grating and the FT-Raman instrument, respectively. Figures 6a and 7a show data recorded from a high-density polymer (density 0.964), Figures 6b and 7b illustrate the spectra obtained from a low-density polymer (density 0.936), and Figures 6c and 7c depict spectra obtained from a very low density polyethylene sample (density 0.904). These spectra show a large variation in band intensity and band shape as a function of density. An example of the curve fitting of the spectrum of the low-density sample recorded on the grating instrument is shown in Figure 8. From this it is corroborated that for the overwhelming part of the spectrum the fitting of the synthesized band profile agrees well with the experimental data. However, as previously stated, the fit around the 1080 cm$^{-1}$ band is considerably more difficult than that in the other regions of the spectrum. The spectra were quantified by using the integrated band areas of the individual components, obtained by integration over a spectral range of 20 times the HWHH of the individual components and using the total area of the 1280–1330 cm$^{-1}$ region for normalization. For quantification we have followed the procedure described by Strobl and Hagedorn.[6] In addition to that method, which uses the 1415 cm$^{-1}$ band to calculate the crystalline content, we have also employed the 1060 cm$^{-1}$ band for that purpose. We have used data obtained from the set of the model alkane compounds to determine the normalization constant ($I_{1060}/I_{1295-1305}$), which was cal-

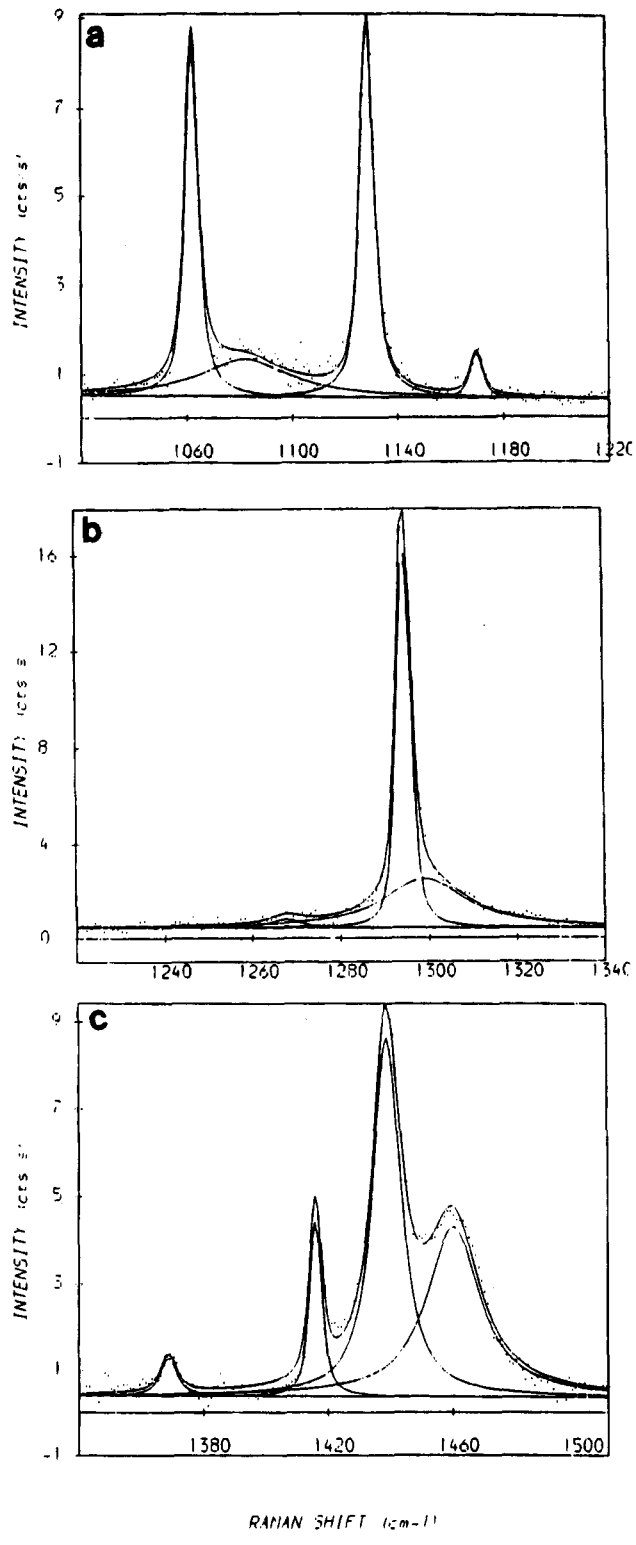


**Figure 8.** Raman spectrum recorded from LDPE, density 0.936 kg/m$^3$, curve fitted with Voigt profiles in three distinct regions.

culated as 0.80 (average value for the model compounds).

Table 2 lists the full range of polyethylene samples we have investigated together with an analysis of their Raman spectra. Closer inspection of these Raman data show that, in general, employing the 1415 cm$^{-1}$ band for calculating the crystallinity, i.e. the Strobl and Hagedorn method, yields differences up to 11% in absolute Raman crystallinities (samples HDPE1, HDPE6, HDPE7) when the results from the grating instrument and the FT-Raman are compared. We note that the agreement is slightly better for crystallinities derived from the 1060 cm$^{-1}$ band (up to 8% difference). It is observed (see, e.g., the data on the "1415" crystallinity) that in some cases the crystallinity obtained from the FT-Raman spectrum is higher than the crystallinity obtained from the Raman spectrum obtained on the grating instrument, while lower in other cases. This suggests that for most of the bands the observed differences are not primarily a result of differences in instrument characteristics but are mainly caused by fitting errors. Moreover, differences of up to 10% were observed when the results obtained using the two different fitting routines applied to the FT-Raman spectra were compared. This discrepancy lies mainly in the problems experienced in fitting the 1280−1330 cm$^{-1}$ region of the spectrum. This region was fitted with two components centered at 1295 and 1305 cm$^{-1}$, respectively. The 1295 cm$^{-1}$ band is a sharp band, while the 1305 cm$^{-1}$ is broad (see Figures 6a and 7a). From these observed differences in crystallinity one can derive a relative uncertainty in the individual band areas of ±5%, which is in general agreement with our experience in fitting this type of spectrum.

Taking into account the mentioned errors, it follows from the data compiled in Table 2 that for the whole series of samples the values for 100 − ("1060" + "1305") are not significantly different from zero. This implies that in case the crystallinity is calculated from the 1060 cm$^{-1}$ band and the amorphous fraction is calculated from the 1305 cm$^{-1}$ band, there is no reason to assume a third, intermediate, phase. In case the crystallinity is calculated from the 1415 cm$^{-1}$ band, the values for 100 − ("1415" + "1305") are also not significantly different from zero from the HDPE samples (samples 1−8). Only in case of LDPE, LLDPE, and VLDPE samples are the values for 100 − ("1415" + "1305") significantly different from zero (values between 9 and 21%). A similar range of values was recently reported by Kennedy et al.[38] who also applied the Strobl and Hagedorn method for quantification of the interfacial content, without the extensive critical analysis we have put forward in the current paper, however. These values might, following Strobl and Hagedorn, be interpretated in terms of a third phase, although this cannot, after our critical evaluation and the doubts that have arisen therefrom, be considered as convincing evidence. In particular, the more difficult fitting of the 1415 cm$^{-1}$ band in the case of lower crystallinity samples, i.e. for the samples of highest "Strobl and Hagedorn third phase", puts more doubts on these values for the low crystallinity samples (LDPE, LLDPE, VLDPE) than for the HPDE samples. In addition, Table 2 also contains crystallinities calculated from density measurements. It can be corroborated from this data set that the crystallinity obtained via the Strobl and Hagedorn method for measuring polyethylene crystallinity, $\alpha_c$, based on the 1415 cm$^{-1}$ Raman band intensity, yields a reasonable correlation with density data only for the higher density polymers. It was found that the crystallinity calculated on the basis of the 1060 cm$^{-1}$ Raman band correlates far better with the crystallinity determined from density than the crystallinity derived from the 1415 cm$^{-1}$ band.

Apart from these considerations there are several other arguments why the application of the Strobl and Hagedorn method for quantification of an interfacial content should be questioned. The Strobl and Hagedorn

method assumes that the Raman spectral features of interest for their analysis are identical for a melt of polyethylene and for the amorphous phase, which is to be considered subject to discussion when we recall the presence of remaining all-trans bands in the melt of polyethylene and the temperature dependence of one of the normalization constants employed within the Strobl and Hagedorn method. Next, there are additional facts that have not been taken into account in any published study including the present study. It is not a priori allowed to assume that similar vibrations have identical Raman scattering cross sections in different phases of polyethylene. In the case of the Strobl and Hagedorn method this is assumed for the "1300 $cm^{-1}$ range". Even within one phase, it is not sure that the Raman scattering cross section does not depend on the more subtle differences in local morphology. In particular, for the low-crystallinity samples (e.g. VLDPE) studied here it was corroborated from WAXS and SAXS experiments that the crystals are very small and imperfect, while the Raman scattering cross section for the 1415 $cm^{-1}$ band could be dependent on the crystallite size.

In conclusion, these observations lead us to conclude that the presence of a third phase in polyethylene on the basis of Raman spectroscopic data has not been demonstrated convincingly, and there is considerable doubt as to whether a third-phase fraction can be abstracted with any reliability from the Raman data.

## Conclusions

The aim of the present study was to verify the method for quantitative determination of a third, interfacial, phase in polyethylene by employing Raman spectroscopy, as first proposed by Strobl and Hagedorn and subsequently used by various other groups. For that purpose Raman spectra were collected on a series of 16 polyethylene samples and a number of model compounds. Measurements were carried out independently in two different laboratories using two different types of Raman spectrometers in order to ensure the correctness of any conclusion. It was shown that once careful attention is paid to the data acquisition parameters and instrument dependent factors, the quantification of data can be made transferable between different types of Raman instrumentation and different laboratories.

The present study revealed that even with sophisticated computer curve-fitting routines the fitting of the bands in the polyethylene spectrum is far from trivial. In particular at the high-density sample range the amorphous features are weak and they are often hard to distinguish from the background signal levels. As a result the normalization value of 0.46 derived by Strobl and Hagedorn to determine the polymer crystallinity was confirmed, while the value of 0.79 relating to the amorphous content was found to vary greatly.

It was suggested to use the 1305 $cm^{-1}$ band for quantifying the amorphous content. This result can be subsequently used for the determination of the fraction of interfacial material according to 100 − ("1415" + "1305"). This approach was found unreliable, for the fraction thus calculated for all 16 polyethylenes (i) provided both positive and negative values, (ii) showed substantial differences between the grating Raman and the FT-Raman data, and (iii) showed differences of similar magnitude upon comparing the results of the application of the two different fitting routines (Voigt and SpectraCalc); see Tables 1 and 2.

These results raise serious doubts as to the current use of Raman spectroscopic data analysis for the calculation of a fraction of the third phase in polyethylene.

**Acknowledgment.** C.N. thanks the COMETT scheme of the EC for financial support. We gratefully acknowledge Steven de Boer for providing the crystallinities as determined by WAXS and Jippe van Ruiten and Vincent Mathot (all DSM Research) for useful discussions. Dr. Organ and Prof. Keller (Bristol University) are acknowledged for providing the $C_{198}H_{398}$ sample. The management of BP Research and the management of DSM Research are acknowledged for their permission to publish this work.

## References and Notes

(1) Mandelkern, L. *Acc. Chem. Res.* **1990**, *23*, 380.
(2) Mandelkern, L. *Chemtracts: Macromol. Chem.* **1992**, *3*, 347.
(3) Bergmann, K.; Nawotki, K. *Koll. Z. Z. Polym.* **1967**, *219*, 132; **1973**, *251*, 962.
(4) Kitamaru, K.; Horii, F.; Hyon, S.-H. *J. Polym. Sci., Polym. Phys.* **1977**, *15*, 821.
(5) Kitamaru, K.; Horii, F. *Adv. Polym. Sci.* **1978**, *26*, 139.
(6) Strobl, G. R.; Hagedorn, W. *J. Polym. Sci., Polym. Phys.* **1978**, *16*, 1181.
(7) Kitamaru, R.; Horri, F.; Murayama, K. *Macromolecules* **1985**, *19*, 636.
(8) Saito, S.; Moteki, Y.; Nakagawa, M.; Horii, F.; Kitamaru, R. *Macromolecules* **1990**, *23*, 3256.
(9) Hirai, A.; Horri, F.; Kitamaru, R.; Fatou, J. G.; Bello, J. G.; *Macrmolecules* **1990**, *23*, 2913.
(10) Earl, W. L.; Vanderhart, D. L. *Macromolecules* **1979**, *12*, 762.
(11) Fisher, E. W. *Polym. J.* **1985**, *17*, 307.
(12) Cheng, S. Z. D.; Wunderlich, B. *Macromolecules* **1988**, *21*, 789.
(13) Cheng, S. Z. D.; Heberer, D. P.; Lieu, H.-S.; Harris, F. W. *J. Polym. Sci., Polym. Phys.* **1991**, *28*, 1896.
(14) Huo, P.; Cebe, P. *Macromolecules* **1192**, *25*, 902.
(15) Huo, P.; Cebe, P. *Colloid Polym. Sci.* **1992**, *270*, 840.
(16) Zachman, H. G.; Stribeck, N.; Alamo, R. G.; Mandelkern, L. Manuscript in preparation.
(17) Mutter, R.; Stille, W.; Strobl, G. *J. Polym. Sci., Polym. Phys.* **1993**, *31*, 99.
(18) Rull F.; Prieto, A. C.; Casado, J. M.; Sobron, F.; Edwards, H. G. M. *J. Raman Spectrosc.* **1993**, *24*, 545.
(19) Marqusee, J. A.; Dill, K. A. *Macromolecules* **1986**, *19*, 2420.
(20) Marqusee, J. A. *Macromolecules* **1989**, *22*, 472.
(21) Kumar, S. K.; Yoon, D. Y. *Macromolecules* **1989**, *22*, 3458.
(22) Nielsen, J. R.; Woollett, *J. Chem. Phys.* **1957**, *26*, 1391.
(23) Boerio, F. J.; Koenig, J. L. *J. Chem. Phys.* **1970**, *52*, 3425.
(24) Gall, M. J.; Hendra, P. J.; Peacock, C. J.; Cudby, M. E.; Willis, H. A. *Spectrochim. Acta* **1972**, *28A*, 1485.
(25) Glotin, M.; Mandelkern, L. *Colloid Polym. Sci.* **1982**, *260*, 182.
(26) Failla, M.; Alamo, R. G.; Mandelkern, L. *Polym. Test.* **1992**, *11*, 151.
(27) Wang, L. H.; Porter, R. S.; Stidham, H. D.; Hsu, S. L. *Macromolecules* **1991**, *24*, 5535.
(28) Keresztury, G.; Földes, E. *Polym. Test.* **1990**, *9*, 329.
(29) Kip, B. J.; Meier, R. J. *Appl. Spectrosc.* **1990**, *44*, 707.
(30) Williams, K. P. J.; Mason, S. M. *Trends Anal. Chem.* **1990**, *9*, 119.
(31) Parker, S. F.; Patel, V.; Tooke, P. B.; Williams, K. P. J. *Spectrochim. Acta* **1991**, *47A*, 1171.
(32) Armstrong, B. H. *J. Quantum Spectrosc. Radiat. Transfer* **1967**, *7*, 61.
(33) Kim, Y.; Strauss, H. L.; Snyder, R. G. *J. Phys. Chem.* **1989**, *93*, 7520.
(34) Mandelkern, L.; Peacock, A. J. *Polym. Bull.* **1986**, *16*, 529.
(35) Snyder, R. G. *J. Chem. Phys.* **1967**, *47*, 1316.
(36) Hagemann, H.; Snyder, R. G.; Peacock, A. J.; Mandelkern, L. *Macromolecules* **1989**, *22*, 3600.
(37) Meier, R. J.; et al. To be submitted.
(38) Kennedy, M. A.; Peacock, A. J.; Mandelkern, L. *Macromolecules* **1994**, *27*, 5297.

MA9412187